Study of coherent population trapping and AC Stark effect in ensembles of NV-centers in diamond at room temperature in microwave range

© R.A. Akhmedzhanov[1], L.A. Gushchin[1], I.V. Zelensky[1]¶, T.G. Mitrofanova[2], V.A. Nizov[1], N.A. Nizov[1], D.A. Sobgaida[1]

[1] Institute of Applied Physics, Russian Academy of Sciences,
603950 Nizhny Novgorod, Russia
[2] Zavoisky Physical-Technical Institute, FRC Kazan Scientific Center of RAS,
420029 Kazan, Russia
¶e-mail: zelensky@appl.sci-nnov.ru

We study coherent population trapping and AC Stark effect using microwave transitions between the sublevels of the ground state of the NV-center. Sublevels with different projections of the nuclear spin of the nitrogen atom are used to implement the Λ-scheme. Dependence of the characteristics of the coherent population trapping dip on the control field frequency and intensity is studied. Various schemes for observing the AC Stark effect are considered.

Keywords: NV-center, coherent population trapping, AC Stark.

Introduction

Interaction between the atom and the light is a fundamental topic in quantum optics and atomic physics. The optical response of a quantum multilevel system can be radically altered by quantum interference between different transitions or by a strong Stark effect. It becomes possible to control the absorption and dispersion of the medium, which opens up a number of promising applications. The effects of electromagnetically induced transparency (EIT), coherent population trapping (CPT) and the AC Stark effect (in a special case, the Autler−Townes effect) have been recently widely discussed. What they have in common is that in all cases a narrow feature appears in the spectral response of the medium. The relative contribution of these effects to the formation of the feature is determined by the intensity of the control field [1]. These phenomena have been actively studied in the optical range [2−4], however, in some media, constructing a Λ-scheme of levels is difficult. For example, in ensembles of NV-centers in diamond, Raman excitation of spin coherence is impossible due to the transitions being symmetry-forbidden. Therefore, the effects of EIT and CPT have been realized to date under conditions of anti-crossing of ground state levels under the effect of a strong external magnetic field [5] and with quasi-zero magnetic fields at internal or external strains corresponding to the anti-crossing of the levels of the first excited state [6]. The situation is much simpler when studying transitions between nuclear spins, when the presence of a relatively small magnetic field oriented at an angle to the axes of the center leads to mixing of nuclear and electron spins, thereby making these transitions allowed [7,8]. This paper presents the results of studies of coherent population trapping (CPT), as well as

the AC Stark effect (the Autler−Townes effect) in various configurations in the microwave range at room temperature.

Coherent population trapping

The effect of coherent population trapping is observed when energy levels form the so-called Λ-scheme — two energy levels connected to a common excited level through allowed transitions. When such a system interacts with two coherent electromagnetic fields with frequencies close to the frequencies of transitions to a common excited level, and two-photon detuning is equal to splitting between the energy levels of the ground state, the system can go into the so-called „dark“ state. This state is a coherent superposition of the ground state levels, and its key feature is that it does not interact with the bichromatic electromagnetic field. As a result, when scanning the frequency of one of the fields and, consequently, two-photon detuning, a dip in the fluorescence profile (or in the absorption spectrum) is observed.

NV-centers in diamond are promising candidates for implementing and observing coherent effects, since transitions between the spin sublevels of the ground state demonstrate a long coherence lifetime even at room temperature. At the same time, NV-centers have a system of energy levels and transitions (Fig. 1, a), in which the spin is polarized by the optical pumping to the sublevel $|0\rangle_s$. As a result, the effect of optical radiation on the spin sublevels can be considered as relaxation of the population of sublevels $|1\rangle_s$ and $|-1\rangle_s$ to the sublevel $|0\rangle_s$ [9,10]. The observed fluorescence is spin-dependent and brighter for the sublevel $|0\rangle_s$. This makes it possible to observe changes in the populations of the sublevels of the ground state, for example, when
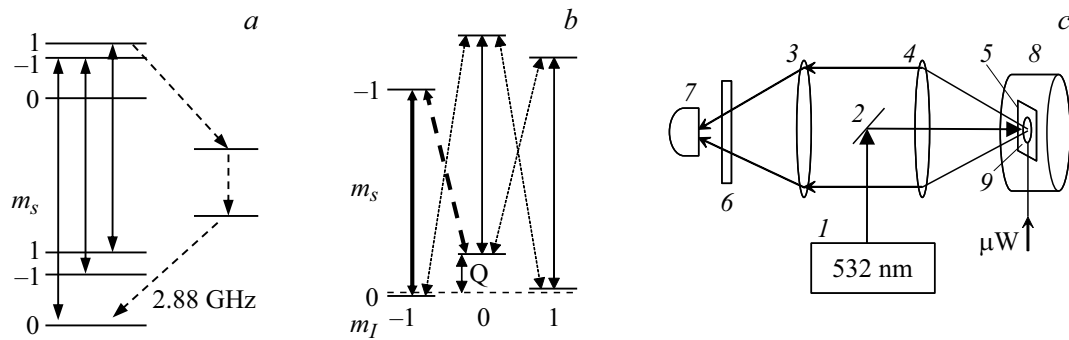
Figure 1. (*a*) The scheme of the electronic levels of the NV-center: solid arrows show optical transitions between the spin sublevels of the ground and excited states, proceeding with the preservation of the spin projection, dashed arrows show an additional relaxation path of the sublevels $m_s = \pm 1$ of the excited state without preserving the spin projection. (*b*) The hyperfine structure of the transition $|0\rangle_S \rightarrow |-1\rangle_S$ between the sublevels of the ground state, dotted lines indicate transitions with changes in nuclear spin, thick lines highlight transitions used to observe the CPT. (*c*) Experimental setup: *1* — laser, *2* — mirror, *3, 4* — lenses, *5* — sample, *6* — light filter, *7* — PMT, *8* — magnetic coil, *9* — antenna.

exposed to microwave radiation, by measuring the fluorescence signal (the optically detectable magnetic resonance method, ODMR).

In the paper [7], the following approach was proposed for observing CPT in the microwave range. Although usually only electron spin levels are considered, each negatively charged NV-center is a system of two connected spins: the spin of an electron and the spin of a nitrogen nucleus. The splittings between the nitrogen spin energy levels are relatively small, and transitions separated by these splittings can be observed in the ODMR profile if the resonances are sufficiently narrow. In zero magnetic fields or fields parallel to the NV-center axis, the projections of the electron and nuclear spins remain good quantum numbers, and transitions with a change in the nuclear spin projection are forbidden. However, the spins have different *g*-factors, so in a field having a component perpendicular to the center axis, the electron and nuclear spin levels become mixed, making transitions that change both spin projections allowed (Fig. 1, *b*). The intensities of these transitions depend on the magnitude and direction of the magnetic field, and, although they usually remain weaker than the direct transitions, the Rabi frequencies can be made equal by adjusting the intensity of the drive and probe fields. The resulting Λ-schemes can be used for the CPT realization experiments. Since ODMR experiments directly use the fact that optical pumping polarizes the electron spin, it is important to note that the magnetic fields required to create Λ-schemes are quite small and only slightly reduce the degree of optical polarization.

Experiment

The splitting between the nuclear spin levels is quite small. In particular, in the zero magnetic field, the levels $|0\rangle_S|-1\rangle_I$ and $|0\rangle_S|0\rangle_I$, used by us to observe the CPT, are split by the value $Q = 4.95$ MHz [11] (splitting is rather
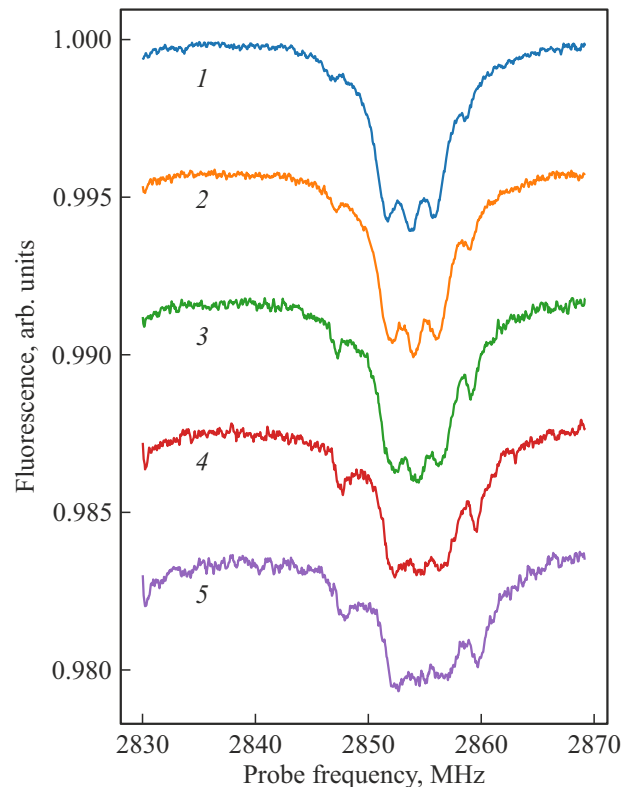
Figure 2. Typical ODMR spectra at different optical pumping intensities: 400 (*1*), 250 (*2*), 160 (*3*), 50 (*4*), 25 mW (*5*). The curves are shifted along the vertical axis for visual clarity.

weakly dependent on the magnetic field, the nuclear *g*-factor is 0.308 kHz/G). Accordingly, in order to resolve the transitions used for CPT, it is necessary to minimize the ODMR linewidth. One of the important factors affecting the linewidth is the quality of the diamond lattice, which decreases with increase in the number of defects. With this in mind, a sample with a low concentration of NV-

centers was made in the diamond electronics laboratory of the Institute of Applied Physics. To do this, a $7\,\mu m$ layer of diamond with a low concentration of NV-centers was grown using CVD (chemical vapor deposition) on the surface of a square substrate made by HPHT (high-pressure high-temperature) method (according to the manufacturer's estimates, the concentration is about $10^{14}\,cm^{-3}$). The direction perpendicular to the surface corresponded to the crystal axis [001], and one of the sides of the square was directed along the axis [110]. The experiment was conducted at room temperature. To collect the fluorescence of NV-centers, a setup assembled in the confocal microscopy configuration was used (Fig. 1, c). Since the concentration of NV-centers was low, the fluorescence intensity was also low. To compensate for the low signal level, sufficiently intense radiation of the pump laser was used (hundreds of mW with a focal spot diameter of about $100\,\mu m$), and a photomultiplier tube was used to register the signal. This system was rather sensitive to background fluorescence and scattered laser light, so a filter with a cutoff wavelength of $650\,nm$ was used to minimize the noise. To observe transitions with a change in the projection of the nuclear spin, an external magnetic field oriented at a large angle to one of the four possible orientations of NV-centers was required. This field was created using a coil placed close to the sample, and the direction and the field strength were adjusted while observing the ODMR profile. The initial resonance, which is a combination of ODMR for the four differently oriented groups of NV-centers, was split by the magnetic field into six separate resonances (for two groups, the angle between the field and the center axis was approximately the same). The resonances that split the least correspond to the largest angle with the direction of the magnetic field, so we worked with this central group of NV-centers in our experiment. According to the calculations based on the positions of the six resonances, the magnetic field was about $35\,G$, and the angle with the axis of the central group of NV-centers was about $75°$ (in these conditions, lifting the ban on transitions with a change in nuclear spin is the most effective [7]). A loop with the diameter of about $3\,mm$ was used as an antenna, and it was pressed against the surface of the sample from the side of the layer containing NV-centers. The laser radiation was focused in the center of the loop. The antenna was powered by two generators (Keysight N5171B and Rohde&Schwartz SMC100A), whose signals, after passing through the isolators that prevent the generators from affecting each other, as well as the passage of the reflected signal, were combined. Since transitions with a change in the projection of the nuclear spin are much weaker than the direct transitions, and the CPT is well observed at equal Rabi frequencies for the transitions forming the Λ-scheme, it was necessary to use high intensity of microwave radiation supplied to the sample. For this purpose, a powerful amplifier (Mini Circuits, ZHL-16W-43-S+) was used, with power up to $16\,W$.

The first step on the way to observing CPT is to find the necessary transitions accompanied by a change in the nuclear spin projection. Typical ODMR spectra of the selected group of NV-centers are shown in Fig. 2. In addition to the main resonance, which is divided into three peaks corresponding to transitions with conservation of nuclear spin $|0\rangle_S|-1\rangle_I \to |-1\rangle_S|-1\rangle_I$, $|0\rangle_S|0\rangle_I \to |-1\rangle_S|0\rangle_I$ and $|0\rangle_S|1\rangle_I \to |-1\rangle_S|1\rangle_I$ (from left to right), smaller peaks can be seen on both sides. These small peaks correspond to transitions with a change in the nuclear spin. The transition $|0\rangle_S|0\rangle_I \to |-1\rangle_S|-1\rangle_I$ is shifted by a value of the order of $Q \approx 5\,MHz$ leftwards of the left main peak. Transitions $|0\rangle_S|1\rangle_I \to |-1\rangle_S|0\rangle_I$ $|0\rangle_S|-1\rangle_I \to |-1\rangle_S|0\rangle_I$ are shifted by $5\,MHz$ from the central main peak to the right and are located close to the right main peak, and cannot be resolved. Theoretically, another transition $|0\rangle_S|0\rangle_I \to |-1\rangle_S|1\rangle_I$ may be observed, shifted by $5\,MHz$ from the right main peak to the left, but under the experimental conditions it is invisible against the background of the nuclear spin preserving transitions. Thus, the transition $|0\rangle_S|0\rangle_I \to |-1\rangle_S|-1\rangle_I$ (the leftmost) is in the most convenient conditions among the nuclear spin changing transitions and together with the transition forming the Λ-scheme with it $|0\rangle_S|-1\rangle_I \to |-1\rangle_S|-1\rangle_I$ (the left main peak) was selected for the CPT observation (Fig. 1, b).

Measurements of the ODMR profiles were carried out (Fig. 2) at different intensities of the optical pumping. It can be seen that the transitions with a change in the spin projection become more noticeable at lower intensities. On the other hand, the ODMR contrast for the direct transitions increases with the increase in optical pumping. This can be explained as follows. Weak optical radiation does not sufficiently polarize the NV-center. As a result, the populations of all levels are nearly equalized both in the presence and in the absence of the microwave field, the contrast is small and increases with increasing pump. On the other hand, if the optical radiation is too strong, the microwave field does not lead to a noticeable redistribution of the population, and the contrast also becomes small. As a result, the ODMR contrast depends nonmonotonically on the intensity of the optical radiation. At first it increases and, having reached a maximum, starts to decrease. At the same time, the intensity of the optical radiation corresponding to the maximum contrast increases with the increase in the Rabi frequency of the microwave field [9]. For transitions not preserving the nuclear spin projection, the Rabi frequency is small (on the order of 10 kHz under the experimental conditions). It can be assumed that the intensities used correspond to the decreasing part of the dependence. For the direct transitions, the Rabi frequency is an order of magnitude higher, so the contrast increases with increasing intensity.

The transition changing the nuclear spin projection $|0\rangle_S|0\rangle_I \to |-1\rangle_S|-1\rangle_I$ was scanned using one of the generators — it was the probe radiation signal. The fluorescence profile was recorded together with the signal of the drive radiation tuned to the transition
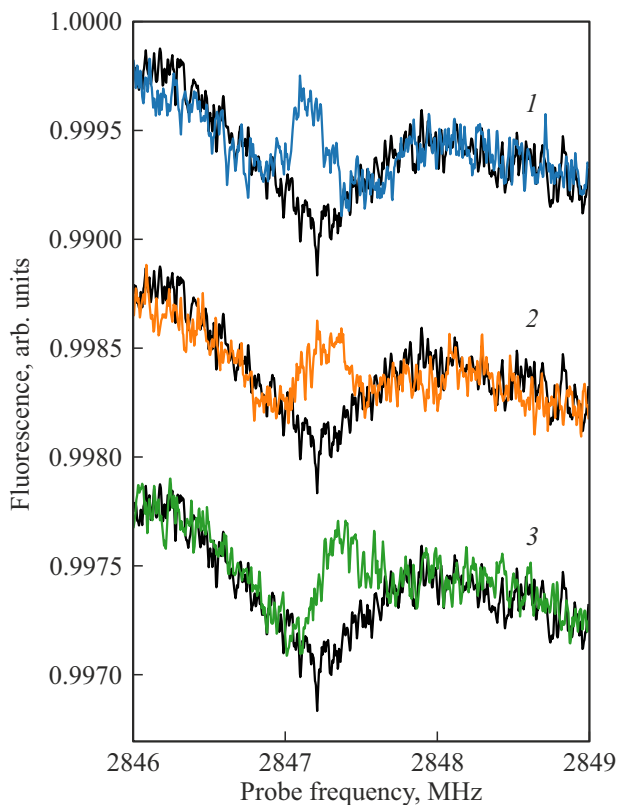
Figure 3. Dependence of the fluorescence signal on the frequency of the probe field at different frequencies of the control field: 2852.1 (*1*), 2852.2 (*2*), 2852.3 MHz (*3*). The signal profile in the absence of the drive field is shown in black.

$|0\rangle_S|-1\rangle_I \rightarrow |-1\rangle_S|-1\rangle_I$, and without it. We chose the maximum intensity of the probe radiation that did not affect the much stronger „direct" transition, and the intensity of the control radiation was chosen so that the Rabi frequencies at the corresponding transitions were approximately equal (about $10-15$ kHz according to our estimates, see below). Typical graphs of the dependence of the fluorescence on the probe field frequency at different frequencies of the drive field are shown in Fig. 3. Turning on the drive field leads to the appearance of a feature in the ODMR spectrum. Due to the coherent population trapping, resonant fields acting at adjacent transitions suppress each other's action. This leads to a decrease in the rate of the population transfer to the common level $|-1\rangle_S|-1\rangle_I$ and, accordingly, an increase in fluorescence. CPT — is a two-photon effect and occurs when the frequency difference of the probe and drive fields is equal to the transition frequency between the lower levels of the Λ-scheme. Accordingly, the position of the feature should shift when the frequency of the drive field changes (in the same direction), as was observed in the experiment. The height and width increase with increasing intensity of the drive field (Fig. 4). In the limit of the low microwave radiation intensities, the width of the CPT resonance is determined by the relaxation rate between the lower levels of the Λ-scheme. The measured value is about 200 kHz

which is quite large and implies high decoherence rates of nuclear spins in our sample.

Another important feature of the system we are investigating is that the rate of population relaxation can be regulated by changing the intensity of the laser pumping, which affects the rate of polarization. However, in the range of intensities available to us, the width and depth of the CPT dip remain unchanged (Fig. 5). It is also seen that the strong optical pumping shifts the position of the transition with the change in the nuclear spin projection to the region of lower frequencies, which can be explained by an increase in the temperature of the sample.
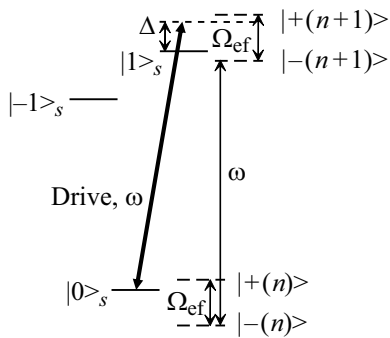
The Autler−Townes Effect

The Autler−Townes effect is a kind of AC Stark effect when a strong oscillating electromagnetic field interacts with a transition between two energy levels. It is convenient to consider this situation in terms of the so-called „dressed states" (Fig. 6). These states form an infinite ladder of pairs of energy levels with a separation determined by the Rabi frequency of the field. The distance between the steps of the stairs is ω, where ω — this is the radiation frequency. When the transition is affected by a non-resonant field, the energy eigenvalues of the Hamiltonian can be written as
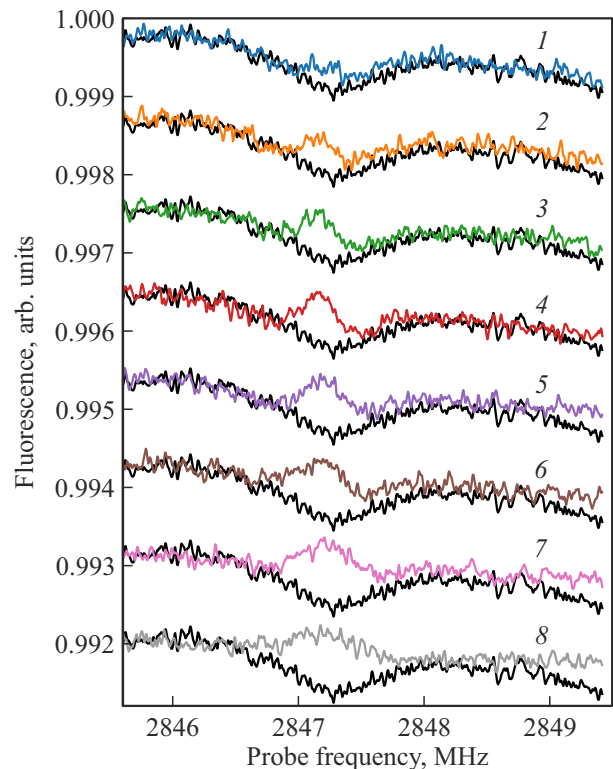
Figure 4. Coherent population trapping spectra at different drive field intensities: -50 (*1*), -45 (*2*), -40 (*3*), -35 (*4*), -30 (*5*), -25 (*6*), -20 (*7*), -15 dBm (*8*). The spectrum in the absence of the drive field is shown in black.
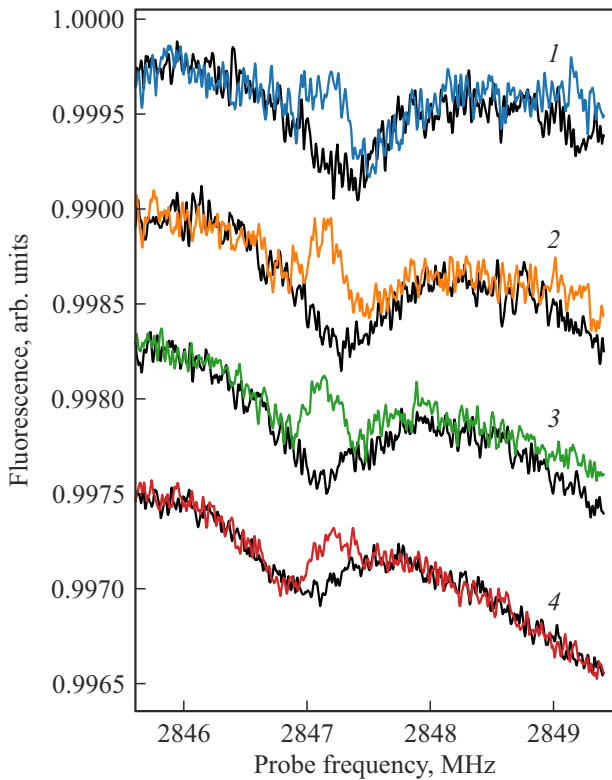
Figure 5. Coherent population trapping spectra at different optical pumping intensities: *1* — 50, *2* — 100, *3* — 160, *4* — 250 mW. The spectrum in the absence of the drive field is shown in black.

Figure 7. ODMR profiles under the influence of the off-resonant field at different frequencies: 2959 (*2*), 2957 (*3*), 2955 MHz (*4*), without off-resonant field (*1*).
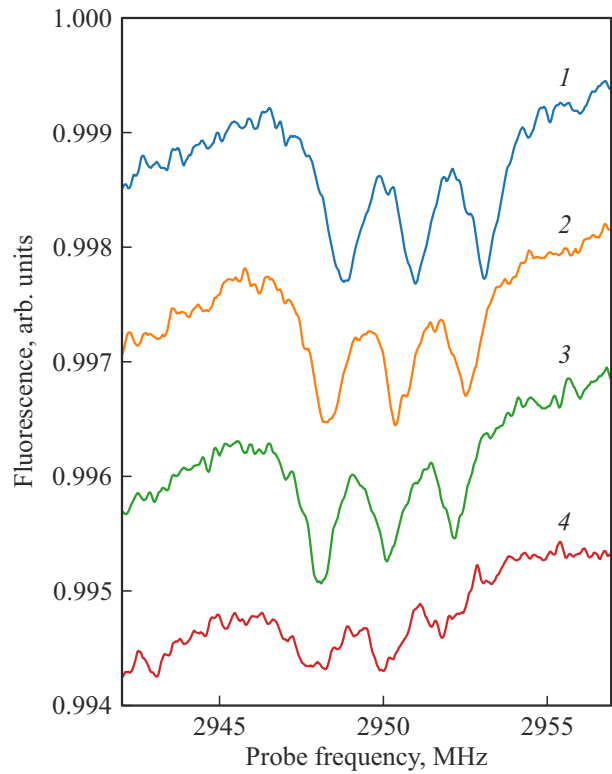

Figure 6. Diagram of the levels of the ground state of the NV-center interacting with the control field, the dashed line shows the „dressed“ states.

follows:

$$E_\pm = \frac{-\hbar\Delta}{2} \pm \frac{\hbar\sqrt{\Omega^2 + \Delta^2}}{2},$$

where Δ — detuning, Ω — Rabi frequency.

The resulting separation between the two levels is equal to the generalized Rabi frequency $\Omega_{ef} = \sqrt{\Omega^2 + \Delta^2}$. With detunings Δ larger than the Rabi frequency, the interaction occurs mainly with the levels close to the undisturbed. In this case, a transition shift is observed. In the case of the resonant interaction, transitions between all levels are possible. When a transition under the effect of a strong exciting field is scanned by a weaker probing field, the fluorescence profile will exhibit three lines known as the Mollow triplet [12]. The position of the center line is determined by the frequency of the control field, and the two side lines are shifted to the generalized Rabi frequency. If the system has a third level with a transition connecting it to one of the two levels affected by the control field, then the splitting between the dressed states can be investigated directly through this transition. In this case, instead of a triplet, only two transitions should be observed. The structure of the NV-center levels allows us to investigate both cases (Fig. 6). It is worth noting that taking into account the hyperfine splitting of the electronic levels (Fig. 1, *b*), the transition scheme turns out to be more complex. Instead of one transition between electronic levels, three are observed (transitions with the nuclear spin preservation, nuclear spin changing transitions are too weak and practically not observed), each of which interacts with the drive field.

Experiment

The setup was similar to that used in the CPT observation experiments. The sample was placed in the same magnetic field to split the electron spin levels and directly investigate the splitting induced by the control field. When the
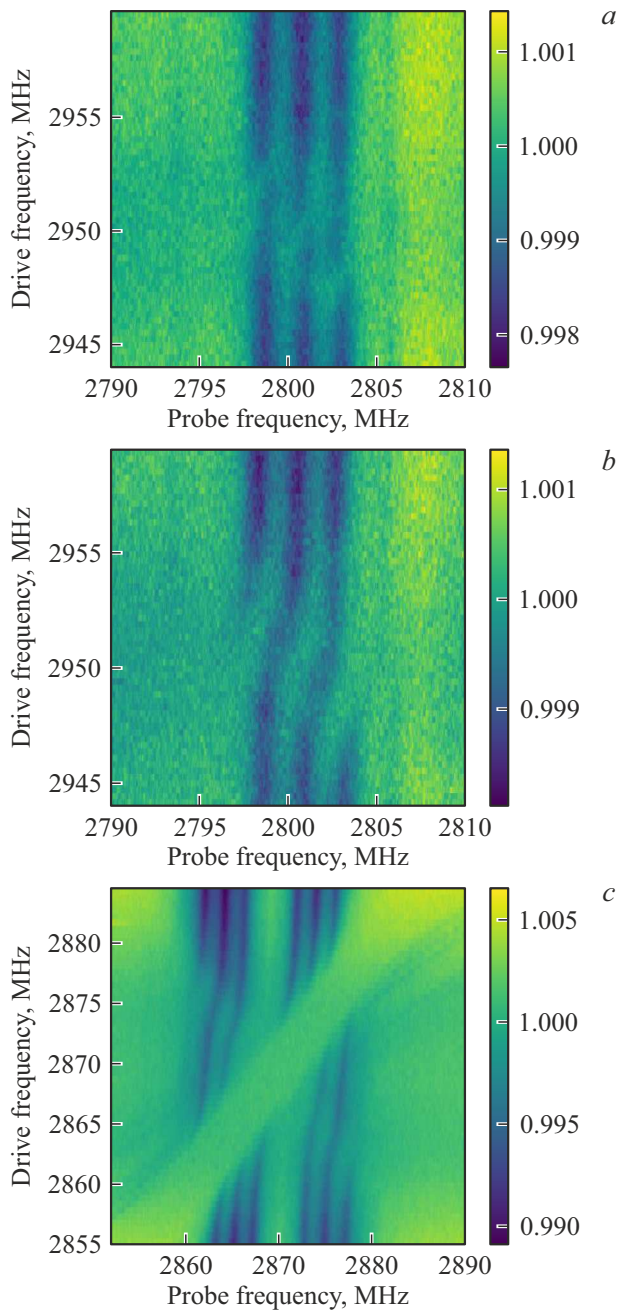
Figure 8. ODMR profiles at the transition $|0\rangle_S \rightarrow |-1\rangle_S$ for different frequencies of the drive field when it passes through the transition $|0\rangle_S \rightarrow |+1\rangle_S$, the Rabi frequency of the drive field (*a*) 1.5 and (*b*) 3 MHz. (*c*) ODMR profiles on transitions $|0\rangle_S \rightarrow |-1\rangle_S$ and $|0\rangle_S \rightarrow |+1\rangle_S$ when the drive field passes through these transitions.

frequency of this field is tuned far enough away from the resonance, it only leads to a shift in the position of the resonance line by the amount of $\Omega^2/2\Delta$ (when $\Delta \gg \Omega$). A similar experiment was carried out using a group of NV-centers with the highest splitting induced by the external magnetic field. The control field was initially tuned approximately 10 MHz away from the resonance, and

then shifted closer. The results are shown in Fig. 7. It can be seen that moving the frequency closer to the transition shifts the resonances further and further, starting to modify their shape as well. These results can be used to estimate the Rabi frequency of the microwave field according to the above formula. According to the data obtained, the signal level of 0 dBm at the output of the generator is approximately equivalent to the Rabi frequency of 3 MHz. This calibration was applied to the results presented in the description of the CPT observation experiment (see above). When the exciting field approaches the resonant frequency, it is expected that the levels involved in the transition form the ladder of dressed states, as discussed above.

To investigate this behavior directly, we conducted an experiment in which the drive field is shifted step-wise (with 275 kHz increments) along the transition $|0\rangle_S \rightarrow |+1\rangle_S$ of the same group, and at each step the spectrum of the ODMR transition $|0\rangle_S \rightarrow |-1\rangle_S$ is recorded. The results for the two different intensities of the drive field are shown in Fig. 8, *a* and *b*. It can be seen that the drive field separates the transition into two parts as it passes through the resonant frequency, while the other lines are shifted. Increasing the intensity of the drive field increases the magnitude of the shifts and splitting. The situation becomes more complicated when the drive field is located at the same transition that is scanned by the probe field. Using a magnetic field oriented so that the transitions of all four orientations of the NV-centers are split equally, we conducted an experiment in which the probing field scans both the transition $|0\rangle_S \rightarrow |-1\rangle_S$ and $|0\rangle_S \rightarrow |+1\rangle_S$, and the frequency of the drive field passes through both transitions in steps of 517 kHz. The results are shown in Fig. 8, *c*. The picture is complicated by the fact that the exciting field in a certain frequency range can be strong enough to affect both transitions simultaneously. It can be seen that the profiles corresponding to the situation when the drive and probe fields act at different transitions are similar to the profiles obtained in the previous experiment (Fig. 8, *a* and *b*), however, the contrast is not high enough to observe the central parts of the Mollow triplet, which should appear when the drive and probe fields act on the same transition.

Conclusion

We investigate the CPT effect in NV-centers in diamond in the microwave range at room temperature. Sublevels of the ground state of the defect corresponding to different projections of the nuclear spin of the nitrogen atom are used. Lifting the ban on transitions not preserving the nuclear spin projection (implementation of the Λ scheme) is carried out by applying an external magnetic field that has a projection perpendicular to the orientation of the NV-center. The dependence of the corresponding CPT dip characteristics in the fluorescence profile on the frequency and intensity of the drive field is investigated.

At room temperature in the microwave range, the AC Stark effect (the Autler−Townes effect) in various configurations is demonstrated. For the orientation of NV-centers selected by an external magnetic field, the dependences of fluorescence on the frequencies of microwave fields are obtained in situations when a strong (drive) field is tuned away from resonance, when the probe and drive fields act on different transitions having a common lower level and when they act on the same transition.

Funding

Conflict of interest

The authors declare that they have no conflict of interest.

References

[1] P.M. Anisimov, J.P. Dowling, B.C. Sanders. Phys. Rev. Lett., **107**, 163604 (2011). DOI: 10.1103/PhysRevLett.107.163604

[2] S.E. Harris. Phys. Today, **50** (7), 36 (1997). DOI: 10.1063/1.881806

[3] M. Fleischhauer, A. Imamoglu, J.P. Marangos. Rev. Mod. Phys., **77**, 633 (2005). DOI: 10.1103/RevModPhys.77.633

[4] N.B. Delone, V.P. Krainov. Phys.-Usp., **42** (7), 669 (1999). DOI: 10.1070/pu1999v042n07ABEH000557.

[5] P.R. Hemmer, A.V. Turukhin, M.S. Shahriar, J.A. Musser. Opt. Lett., **26** (6), 361 (2001). DOI: 10.1364/OL.26.000361

[6] V.M. Acosta, K. Jensen, C. Santori, D. Budker, R.G. Beausoleil. Phys. Rev. Lett., **110**, 213605 (2013). DOI: 10.1103/PhysRevLett.110.213605

[7] P. Huillery, J. Leibold, T. Delord, L. Nicolas, J. Achard, A. Tallaire, G. Hétet. Phys. Rev. B, **103**, L140102 (2021). DOI: 10.1103/PhysRevB.103.L140102

[8] P. Jamonneau, G. Hétet, A. Dréau, J.-F. Roch, V. Jacques. Phys. Rev. Lett., **116**, 043603 (2016). DOI: 10.1103/PhysRevLett.116.043603

[9] K. Jensen, V.M. Acosta, A. Jarmola, D. Budker. Phys. Rev. B, **87**, 014115 (2013). DOI: 10.1103/PhysRevB.87.014115

[10] A. Dréau, M. Lesik, L. Rondin, P. Spinicelli, O. Arcizet, J.-F. Roch, V. Jacques. Phys. Rev. B, **84**, 195204 (2011). DOI: 10.1103/PhysRevB.84.195204

[11] B. Smeltzer, J. McIntyre, L. Childress. Phys. Rev. B, **80**, 050302(R) (2009). DOI: 10.1103/PhysRevA.80.050302

[12] H. Morishita, T. Tashima, D. Mima, H. Kato, T. Makino, S. Yamasaki, M. Fujiwara, N. Mizuochi. Sci. Rep., **9**, 13318 (2019). DOI: 10.1038/s41598-019-49683-z